Supplementary Materials:

Straight versus branched chain substituents in 4'-(butoxyphenyl)-3,2':6',3"-terpyridines: Effects on (4,4) coordination network assemblies

Dalila Rocco [1], Alessandro Prescimone [1], Edwin C. Constable [1] and Catherine E. Housecroft [1]*

[1] Department of Chemistry, University of Basel, BPR 1096, Mattenstrasse 24a, CH-4058 Basel, Switzerland; dalila.rocco@unibas.ch (D.R.); alessandro.prescimone@unibas.ch (A.P.); edwin.constable@unibas.ch (E.C.C.), catherine.housecroft@unibas.ch (C.E.H.)

* Correspondence: catherine.housecroft@unibas.ch; Tel: +41 61 207 1008

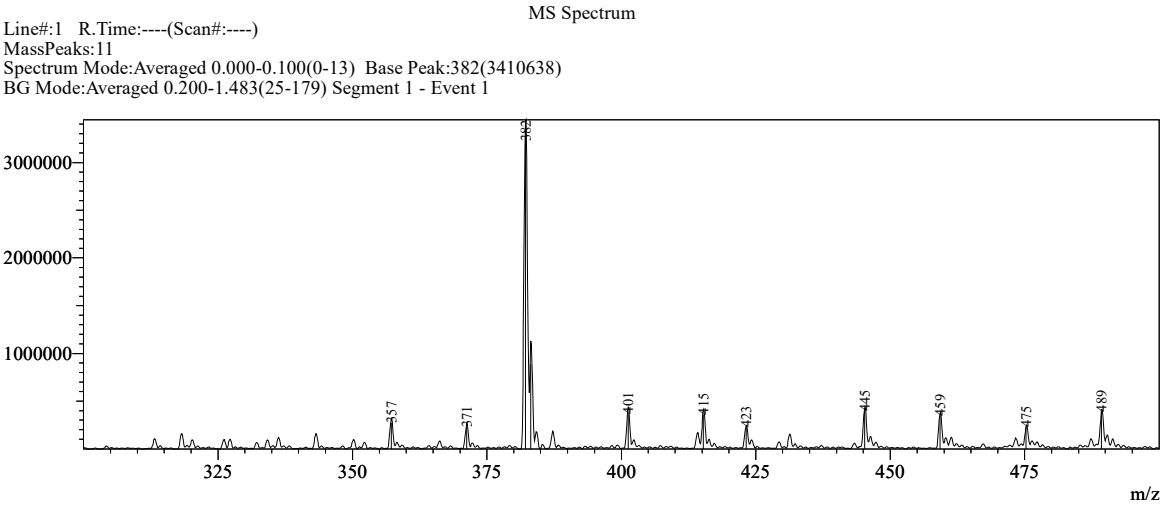

Figure. S1. Electrospray mass spectrum of *rac*-**2**.

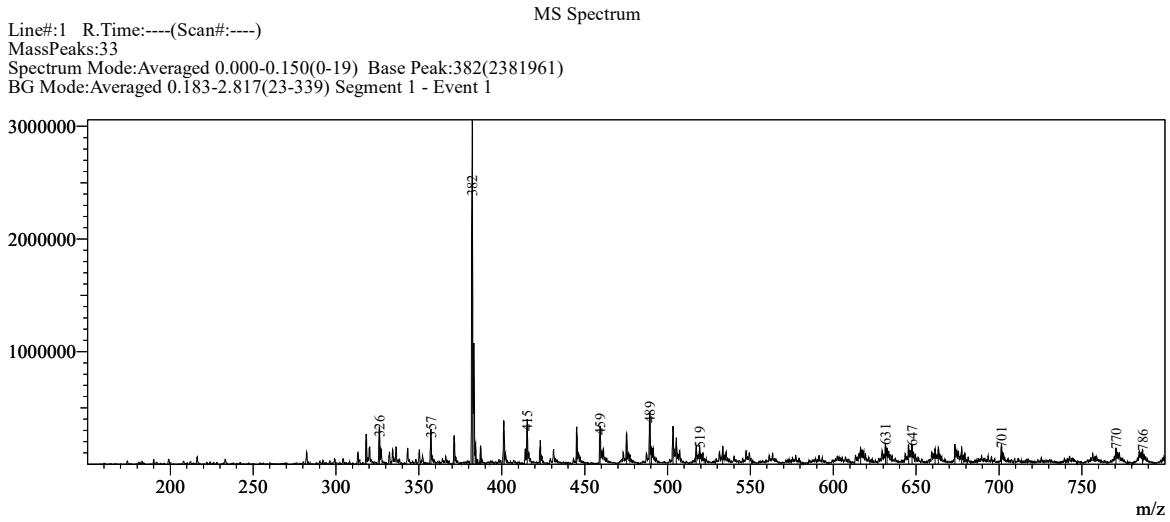

Figure. S2. Electrospray mass spectrum of **4**.

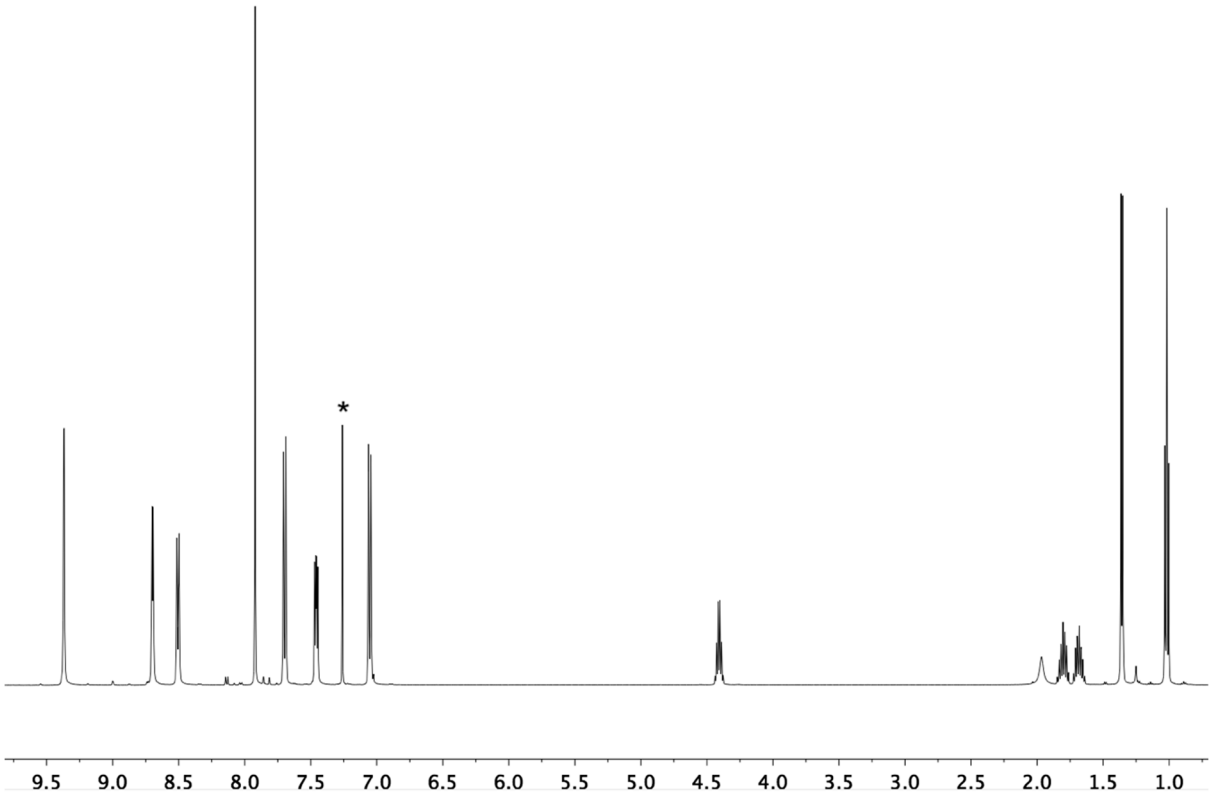

Figure. S3. ^{1}H NMR spectrum of compound *rac*-**2** (500 MHz, 298 K, $CDCl_3$). * = residual $CHCl_3$.

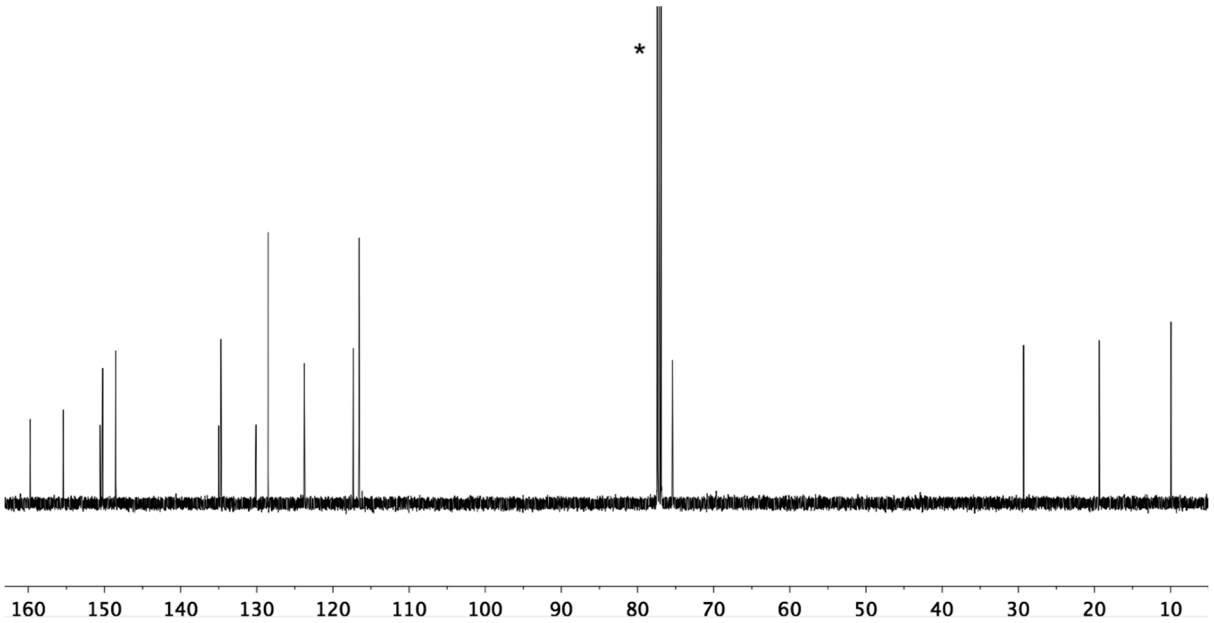

Figure. S4. $^{13}C\{^{1}H\}$ NMR spectrum of compound *rac*-**2** (126 MHz, 298 K, $CDCl_3$). * = $CDCl_3$.

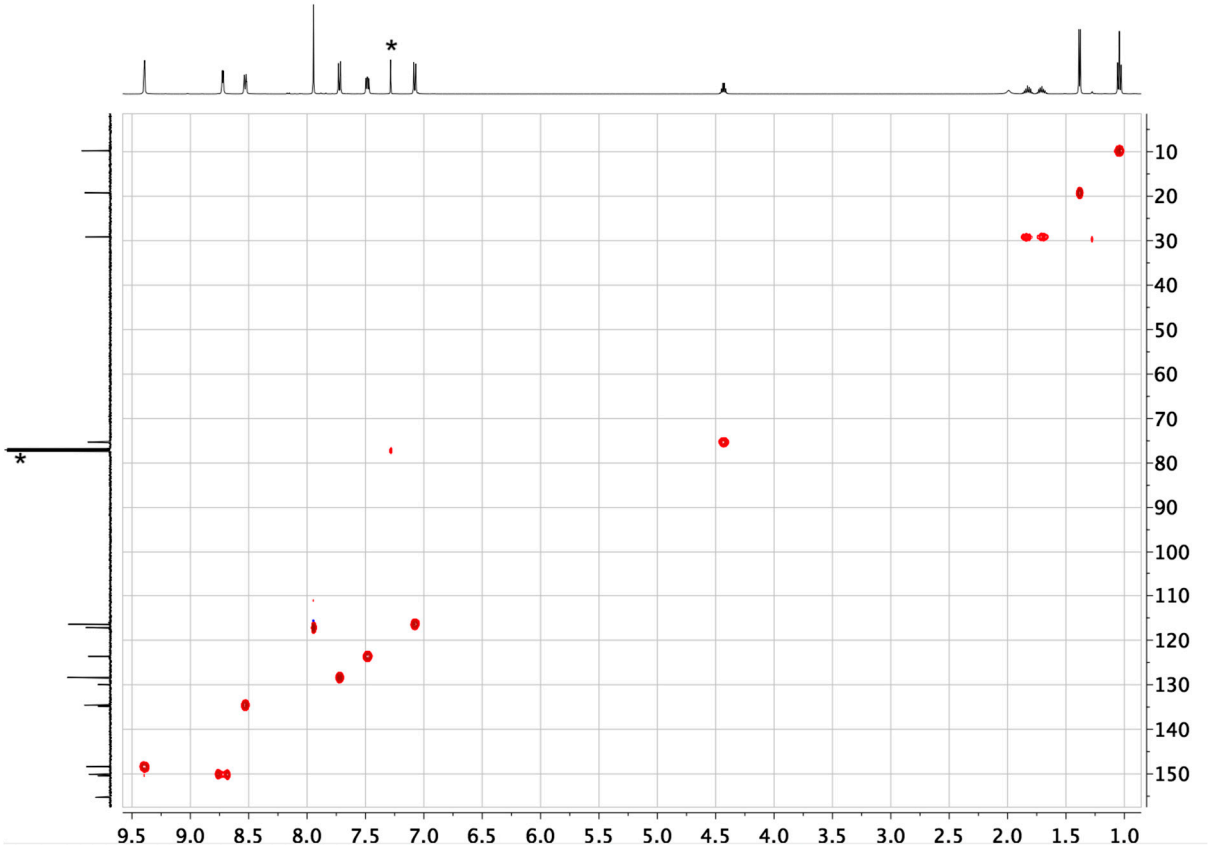

Figure. S5. HMQC spectrum of compound *rac*-**2** (^{1}H 500 MHz, ^{13}C 126 MHz, 298 K, $CDCl_3$). * = residual $CHCl_3$ or $CDCl_3$.

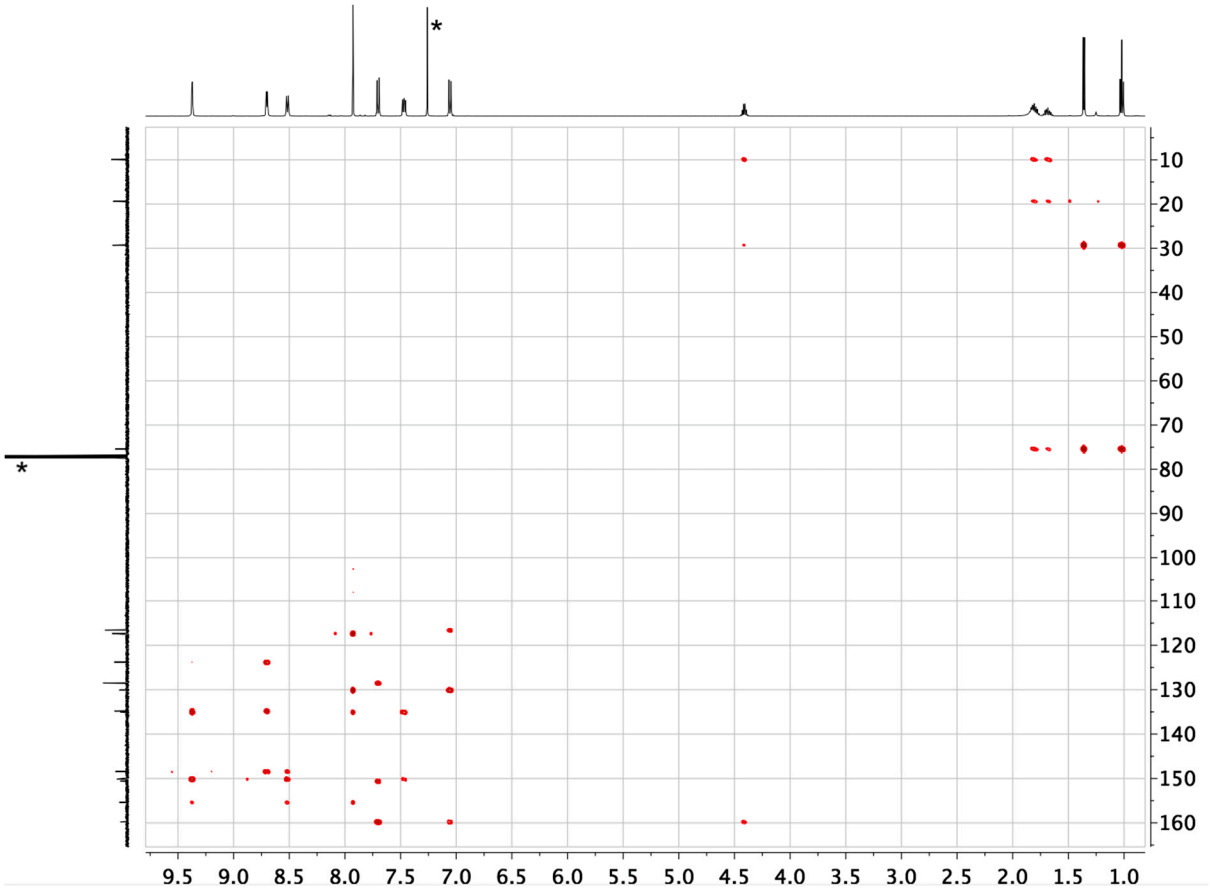

Figure. S6. HMBC spectrum of compound *rac*-**2** (^{1}H 500 MHz, ^{13}C 126 MHz, 298 K, $CDCl_3$). * = residual $CHCl_3$ or $CDCl_3$.

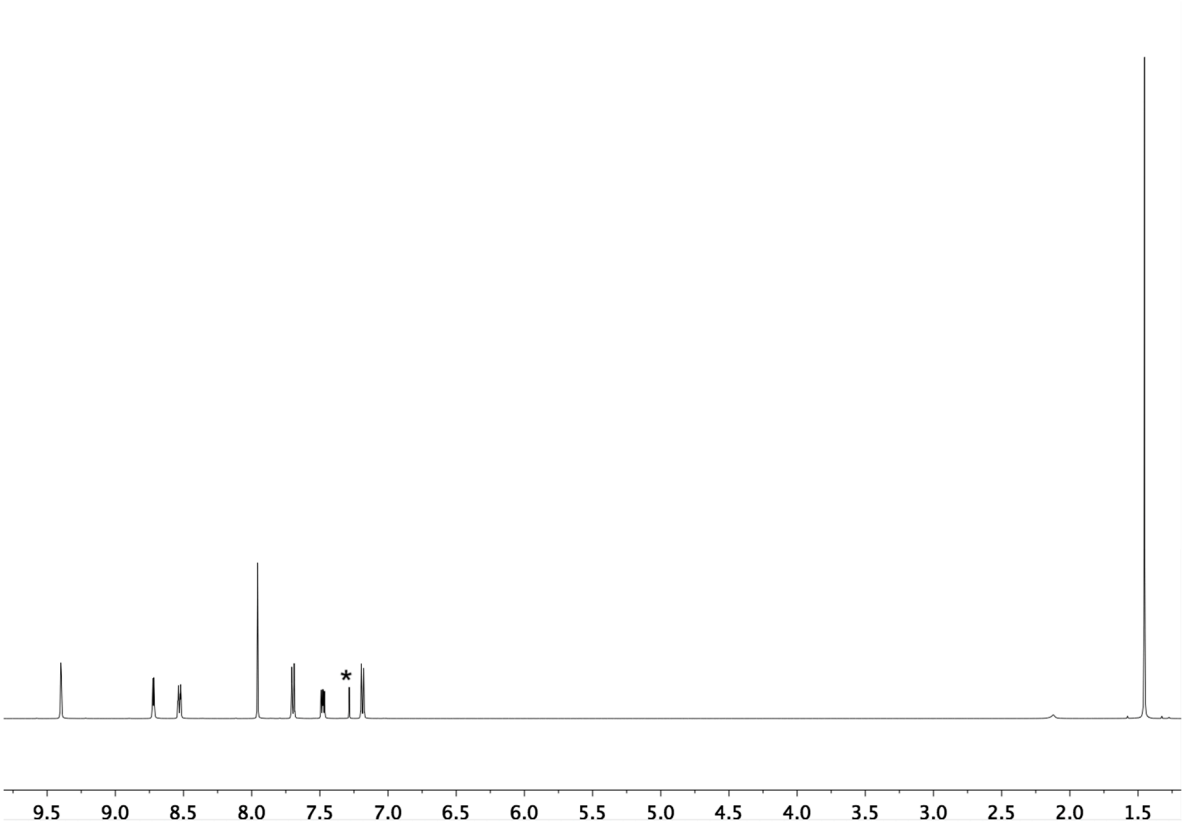

Figure. S7. ^{1}H NMR spectrum of compound **4** (500 MHz, 298 K, $CDCl_3$). * = residual $CHCl_3$.

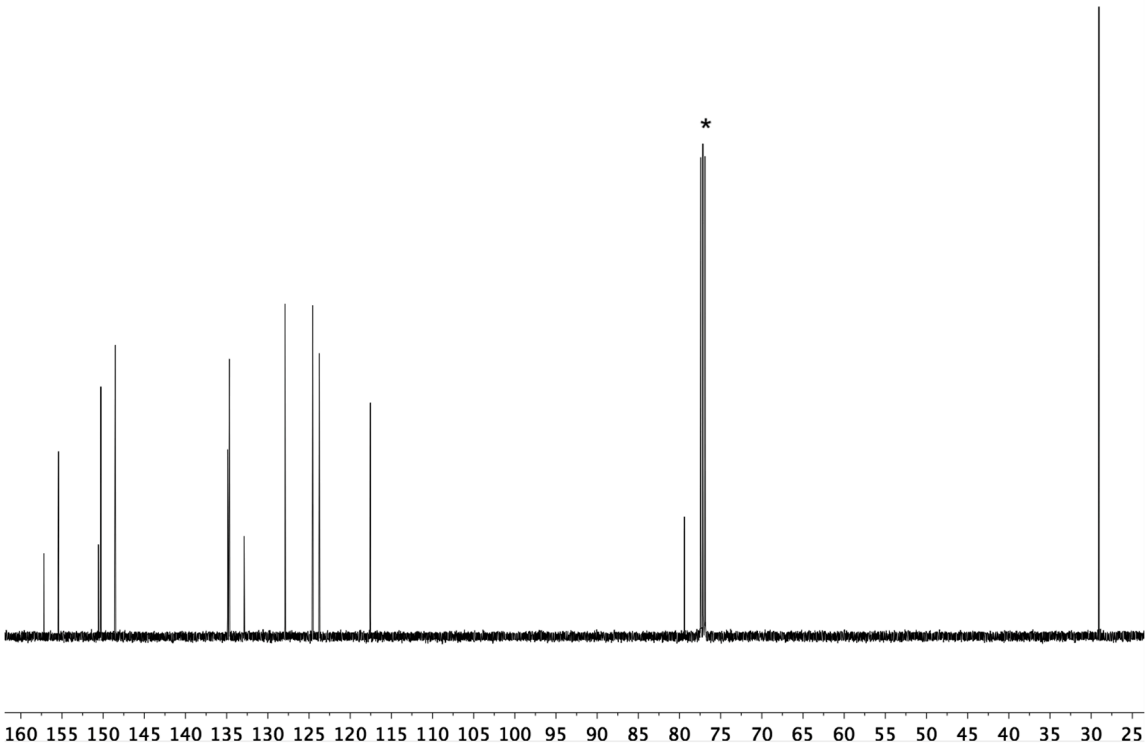

Figure. S8. $^{13}C\{^{1}H\}$ NMR spectrum of compound **4** (126 MHz, 298 K, $CDCl_3$). * = $CDCl_3$.

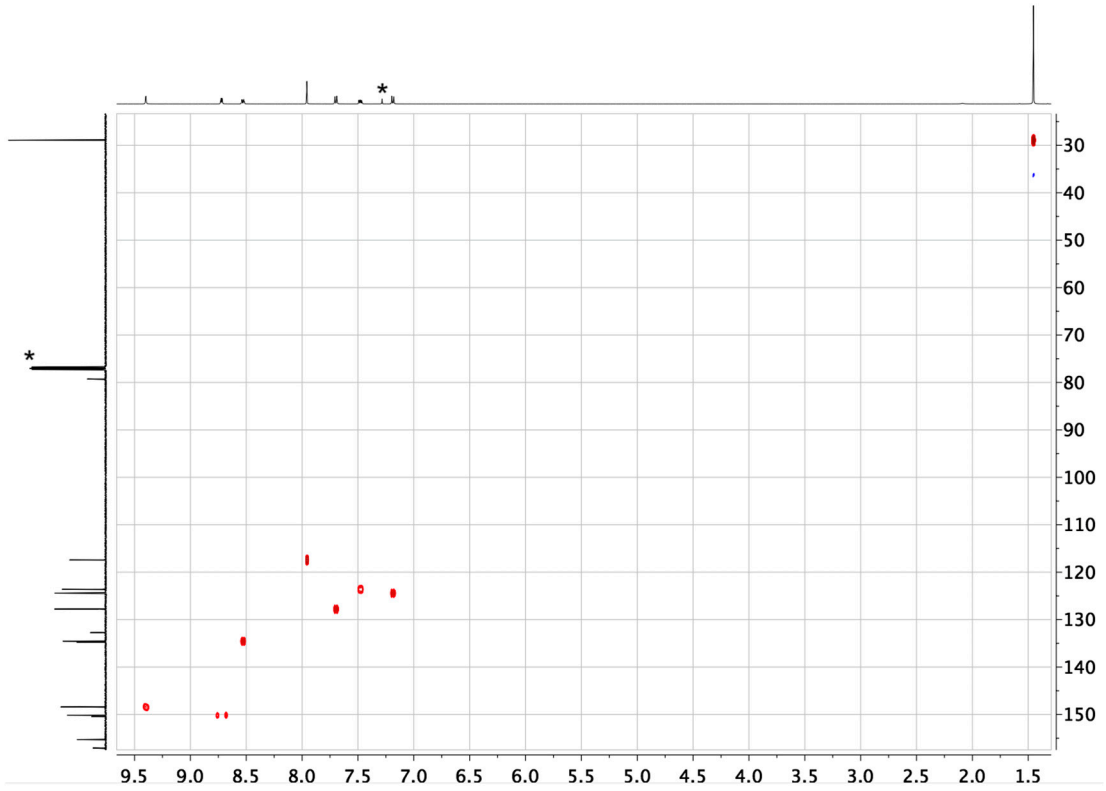

Figure. S9. HMQC spectrum of compound **4** (^{1}H 500 MHz, ^{13}C 126 MHz, 298 K, $CDCl_3$). * = residual $CHCl_3$ or $CDCl_3$.

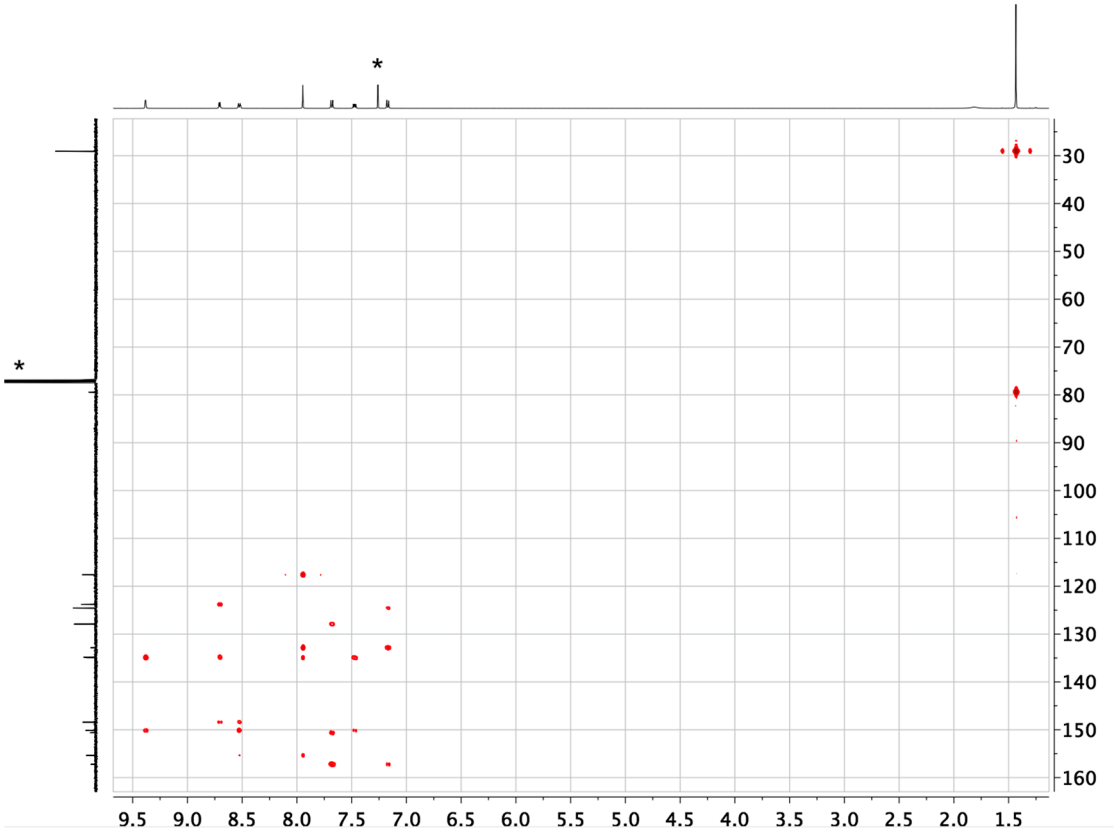

Figure. S10. HMBC spectrum of compound **4** (^{1}H 500 MHz, ^{13}C 126 MHz, 298 K, $CDCl_3$). * = residual $CHCl_3$ or $CDCl_3$.

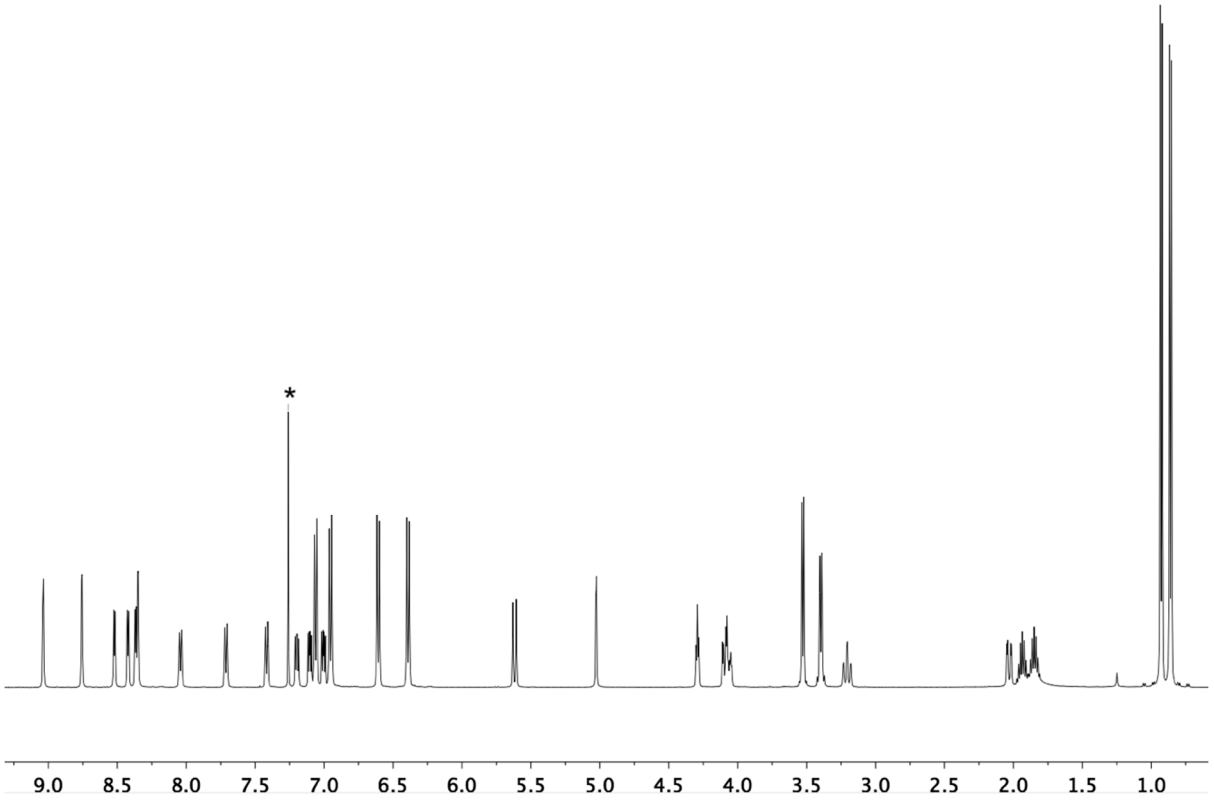

Figure. S11. ^{1}H NMR spectrum of compound **3a** (500 MHz, 298 K, $CDCl_3$). * = residual $CHCl_3$.

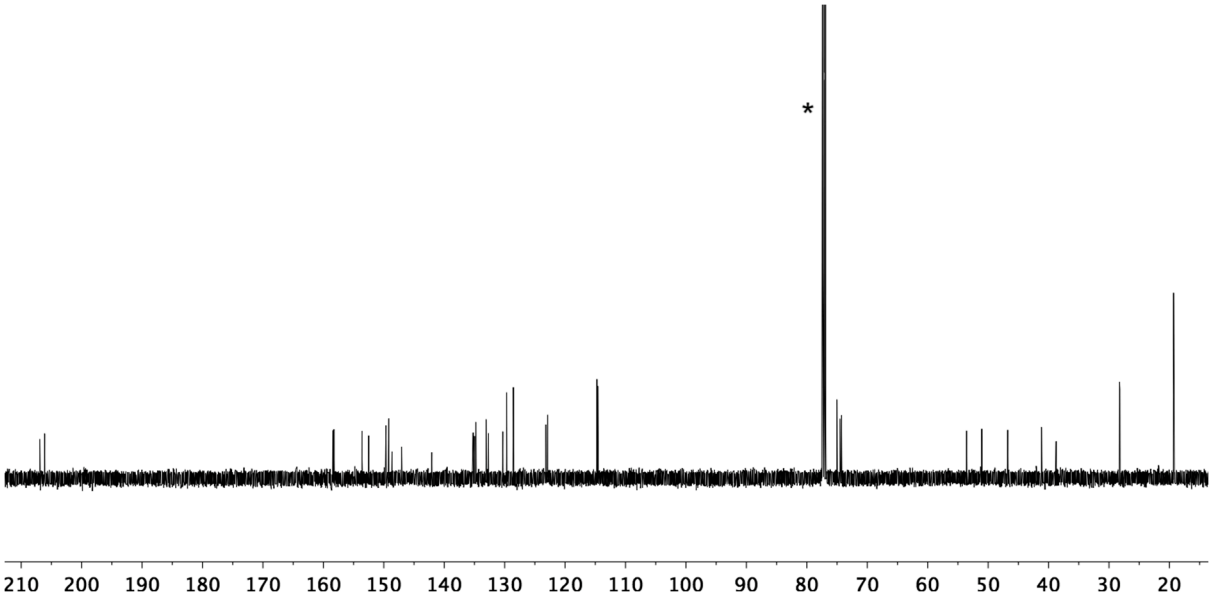

Figure. S12. $^{13}C\{^{1}H\}$ NMR spectrum of compound **3a** (126 MHz, 298 K, $CDCl_3$). * = $CDCl_3$.

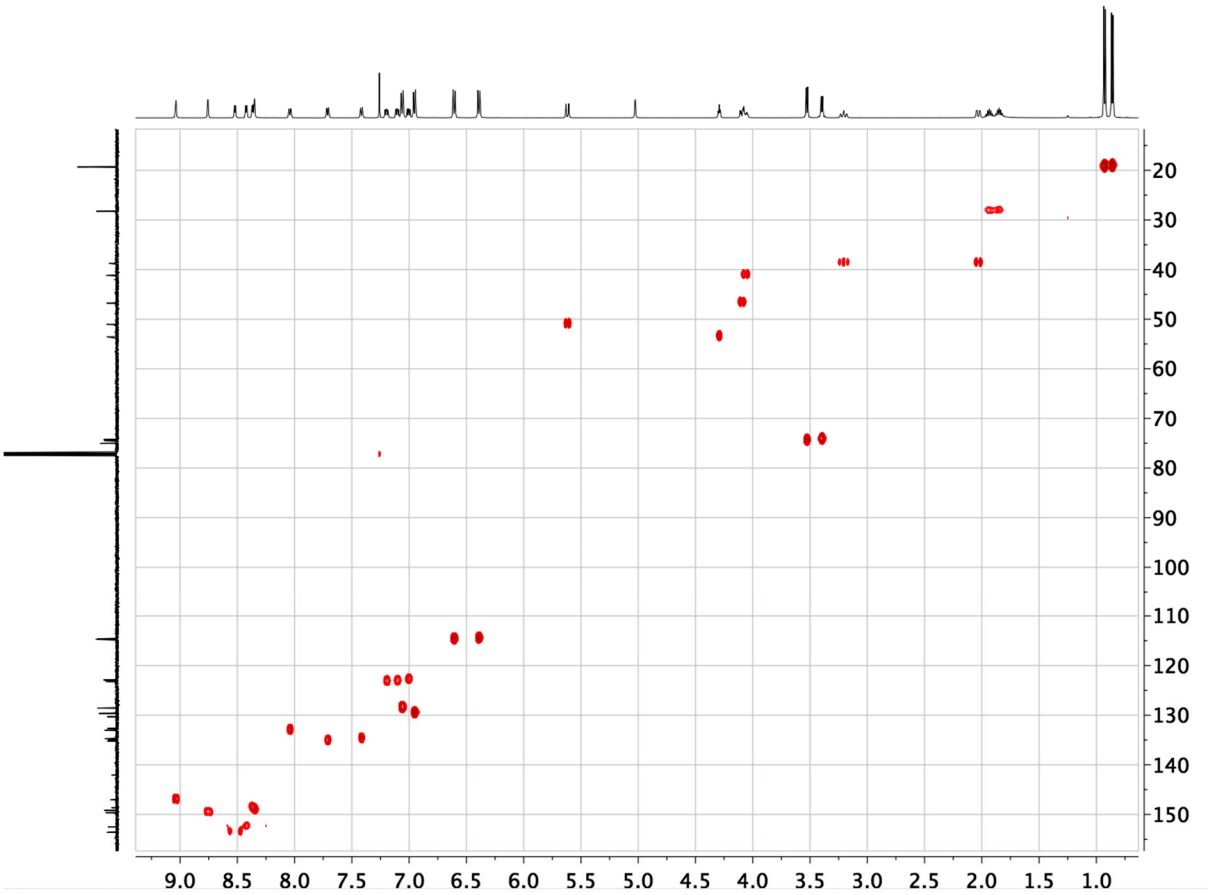

Figure. S13. HMQC spectrum of compound **3a** (^{1}H 500 MHz, ^{13}C 126 MHz, 298 K, $CDCl_3$). * = residual $CHCl_3$ or $CDCl_3$.

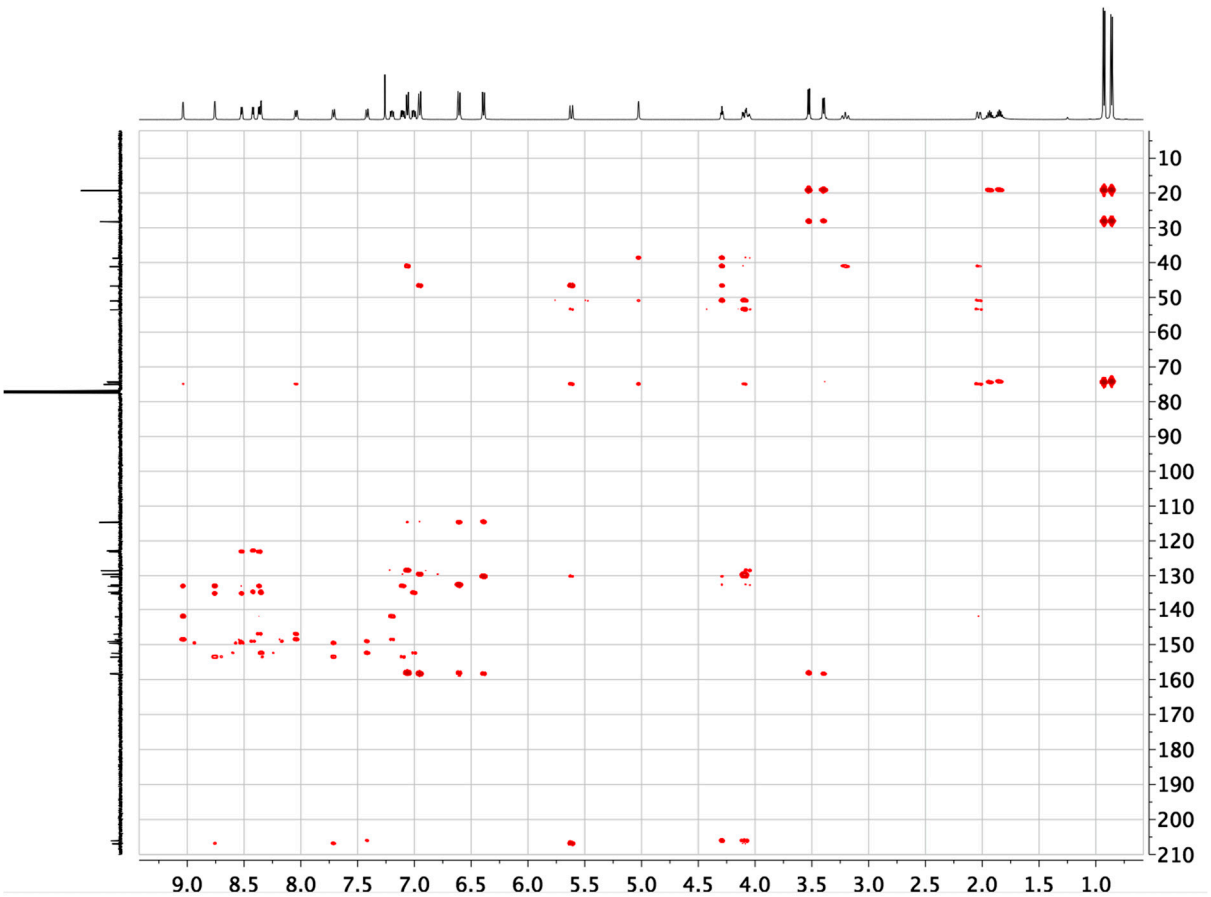

Figure. S14. HMBC spectrum of compound **3a** (^{1}H 500 MHz, ^{13}C 126 MHz, 298 K, $CDCl_3$). * = residual $CHCl_3$ or $CDCl_3$.

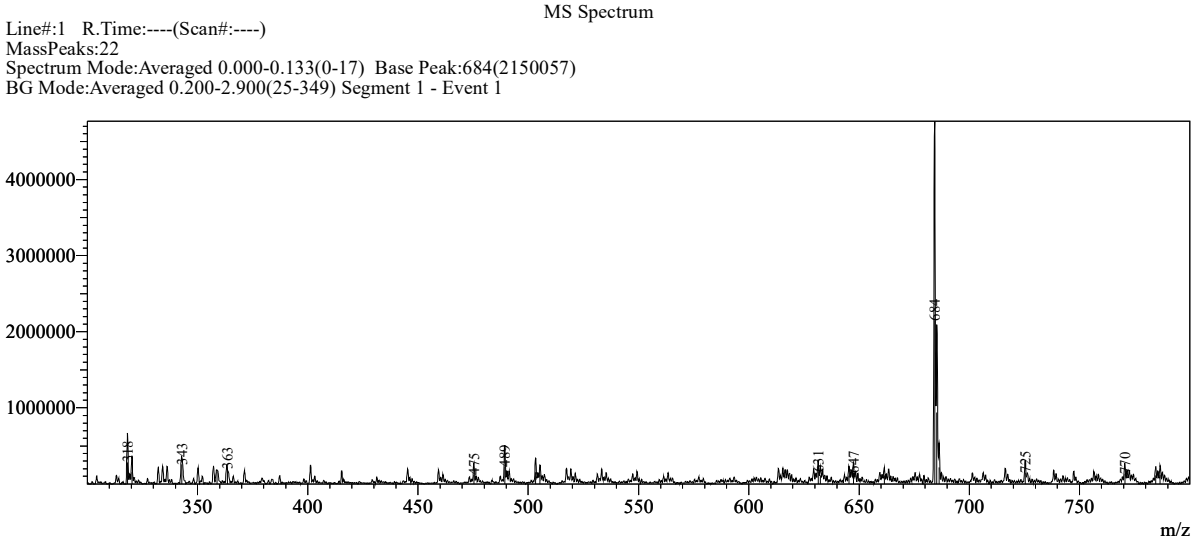

Figure. S15. Electrospray mass spectrum of compound **3a**.

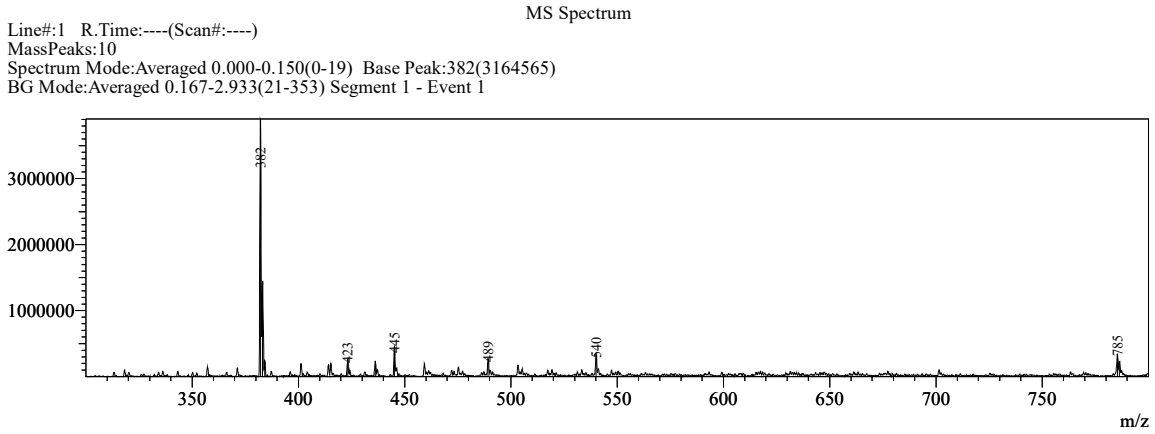

Figure. S16. Electrospray mass spectrum of compound **3**.

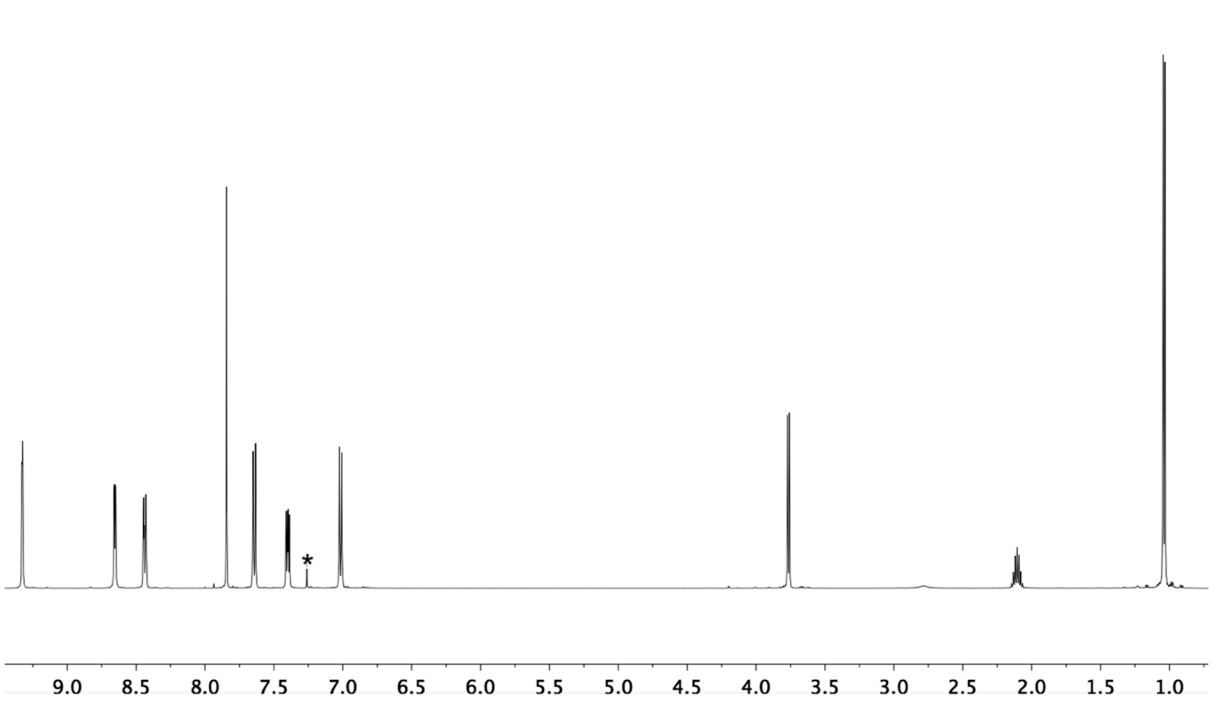

Figure. S17. ^{1}H NMR spectrum of compound **3** (500 MHz, 298 K, $CDCl_3$). * = residual $CHCl_3$.

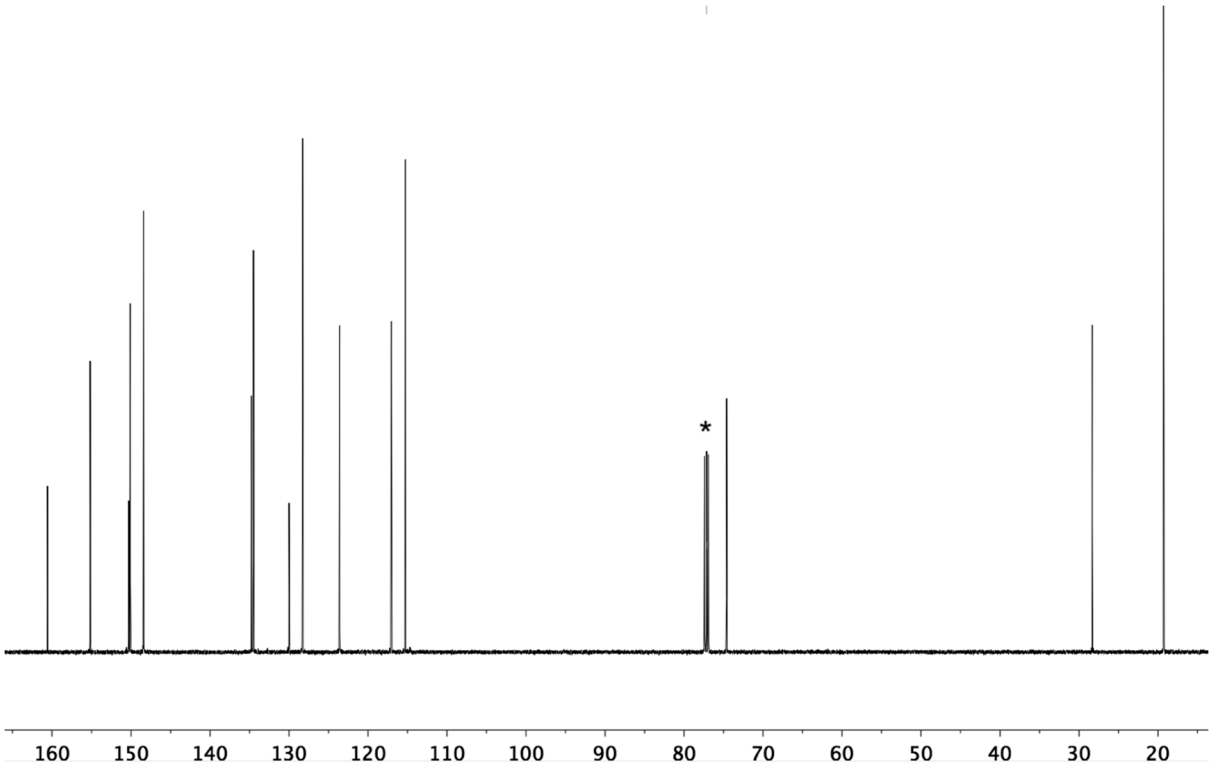

Figure. S18. $^{13}C\{^{1}H\}$ NMR spectrum of compound **3** (126 MHz, 298 K, $CDCl_3$). * = $CDCl_3$.

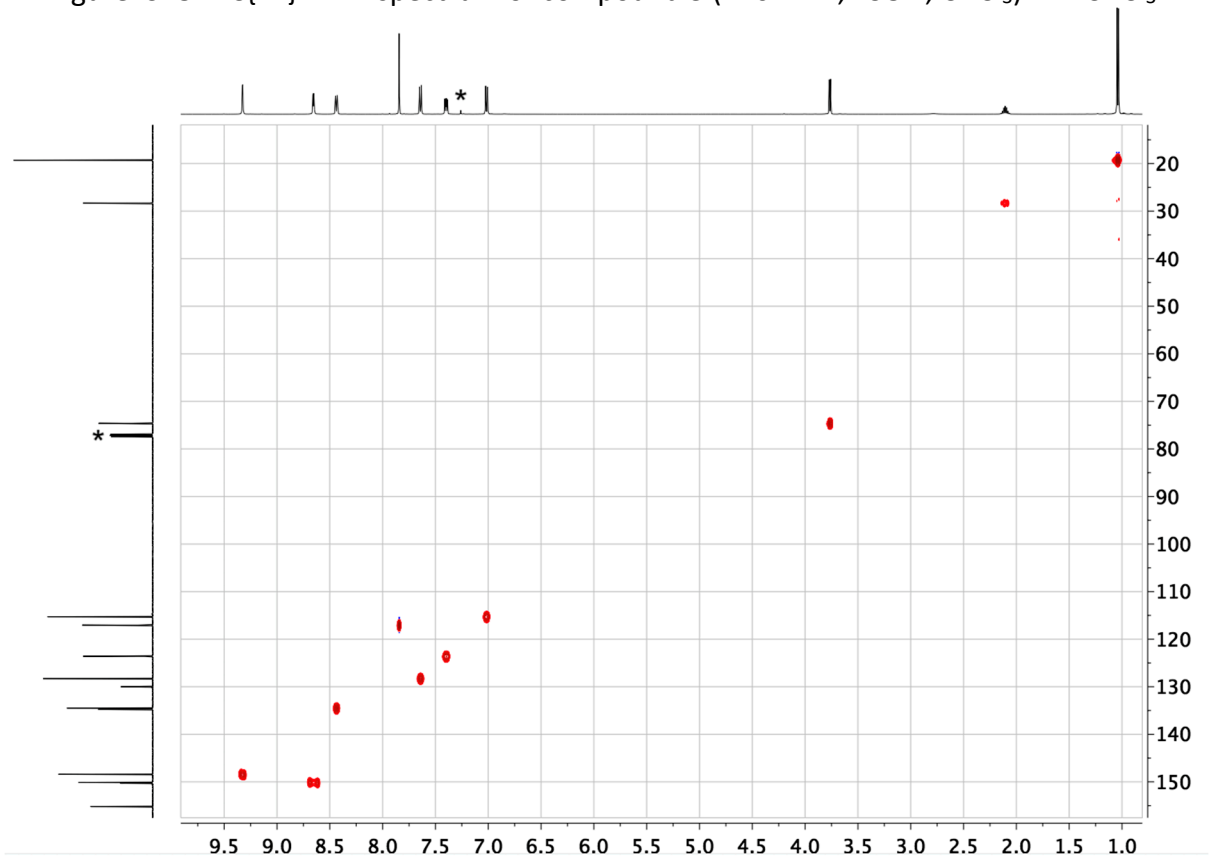

Figure. S19. HMQC spectrum of compound **3** (^{1}H 500 MHz, ^{13}C 126 MHz, 298 K, $CDCl_3$). * = residual $CHCl_3$ or $CDCl_3$.

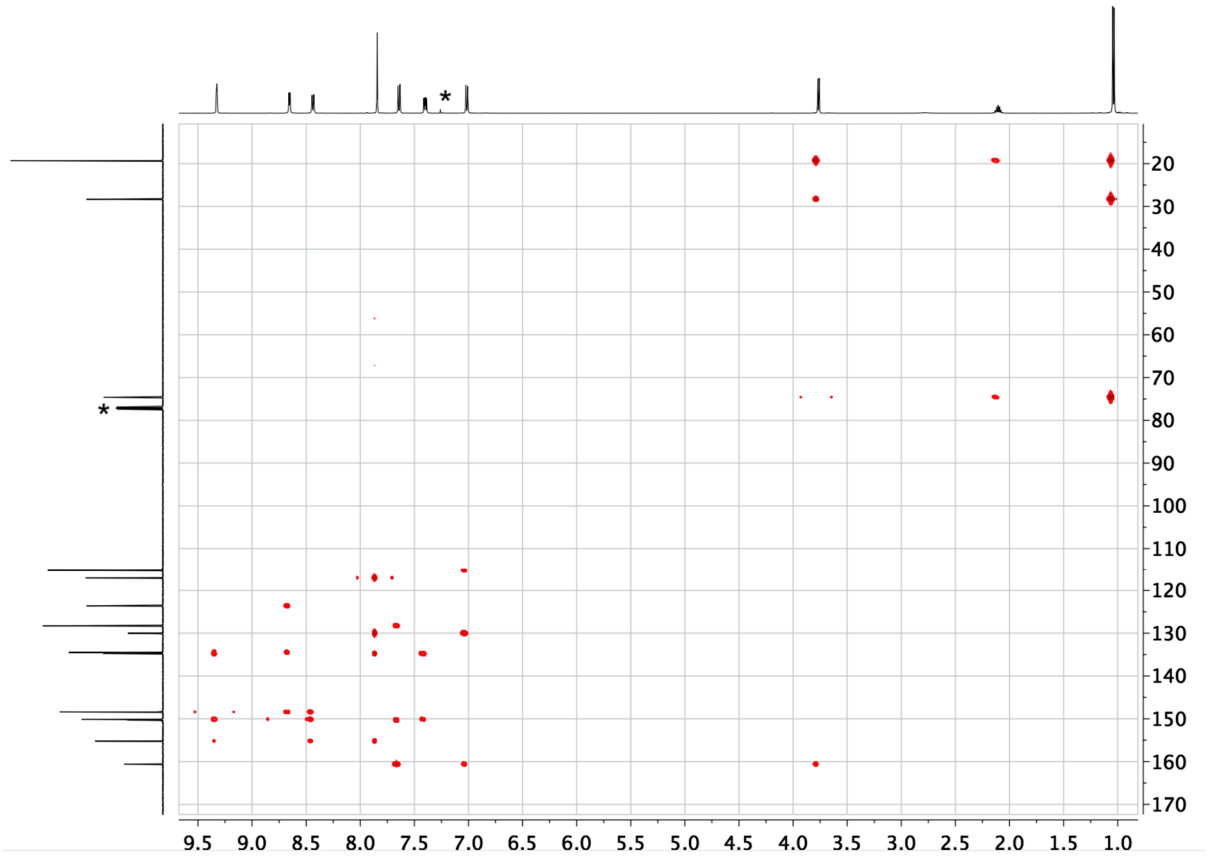

Figure. S20. HMBC spectrum of compound **3** (^{1}H 500 MHz, ^{13}C 126 MHz, 298 K, $CDCl_3$). * = residual $CHCl_3$ or $CDCl_3$.

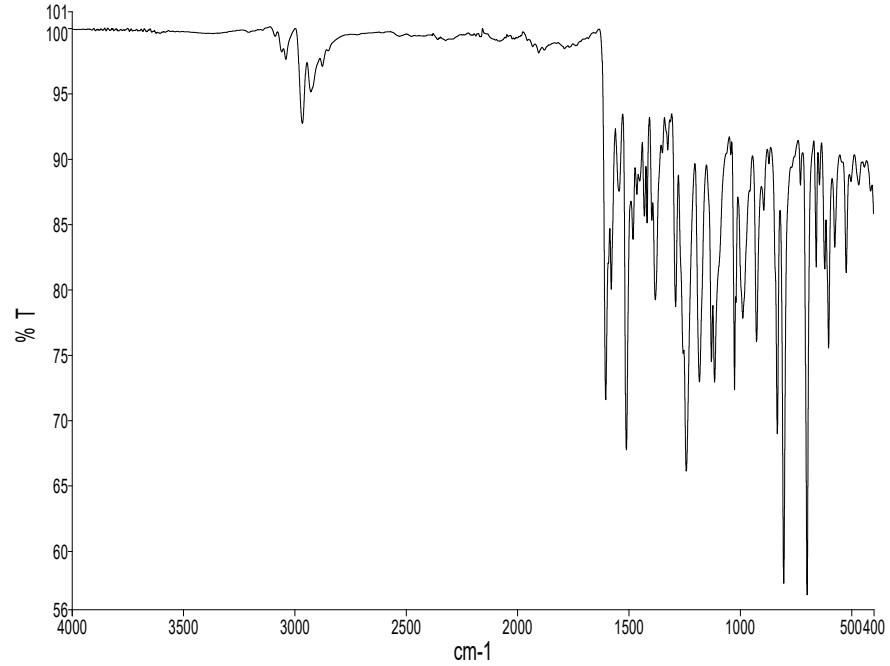

Figure. S21. The solid-state FT-IR spectrum of *rac*-**2**.

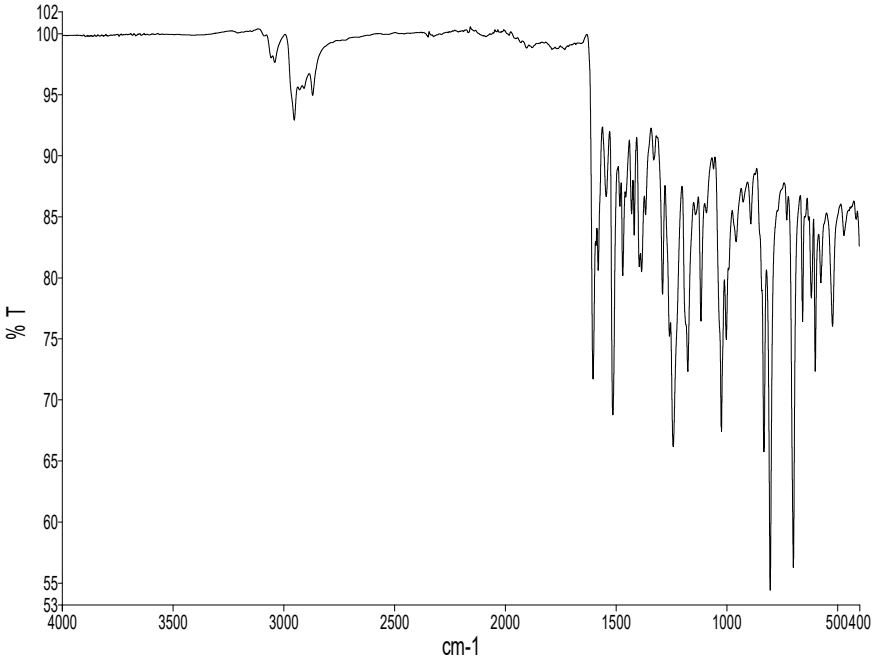

Figure. S22. The solid-state FT-IR spectrum of **3**.

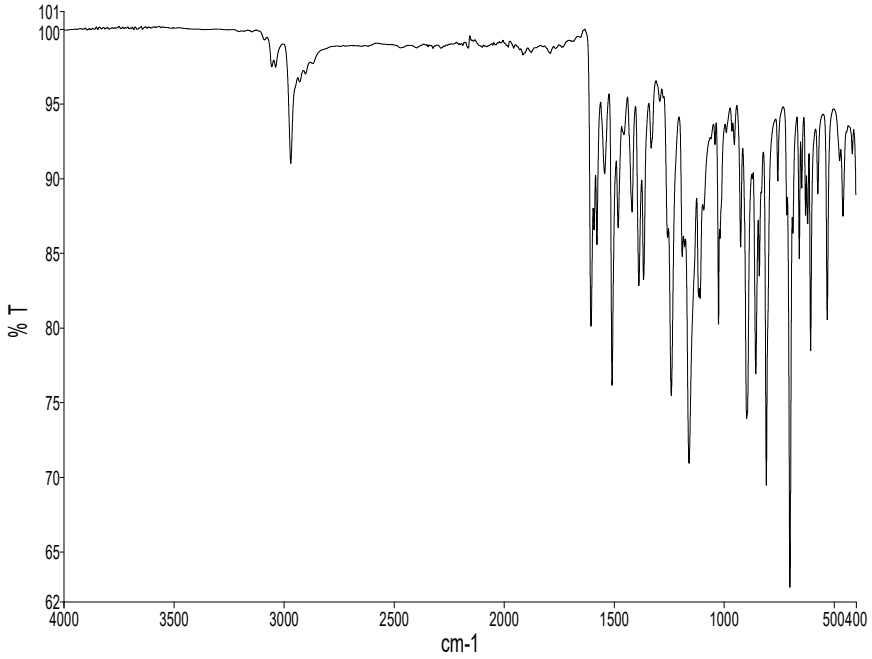

Figure. S23. The solid-state FT-IR spectrum of **4**.

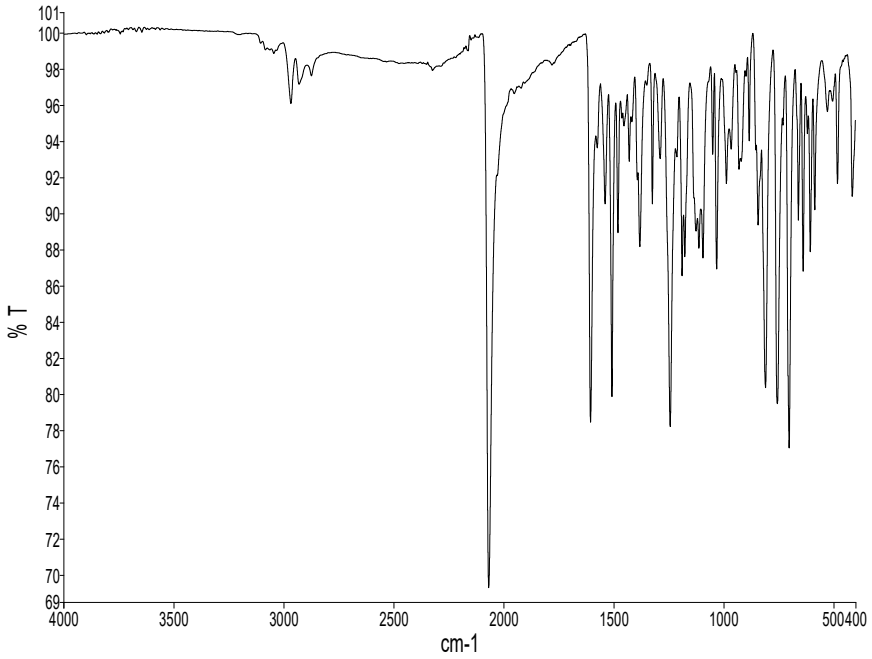

Figure. S24. The solid-state FT-IR spectrum of [{Co(*rac*-**2**)$_2$(NCS)$_2$}·CHCl$_3$]$_n$.

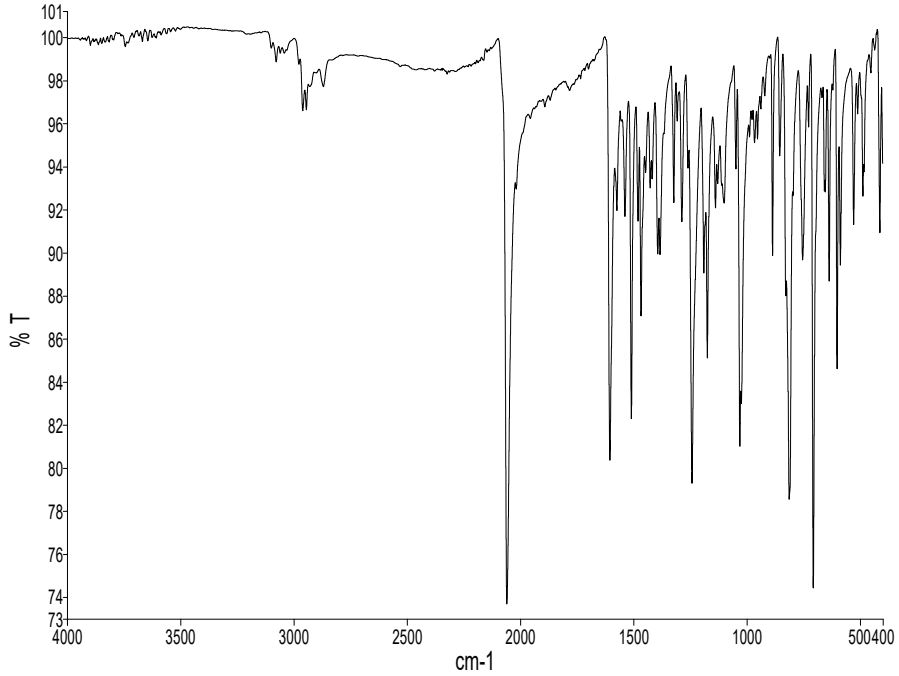

Figure. S25. The solid-state FT-IR spectrum of [{Co(**3**)$_2$(NCS)$_2$}]$_n$.

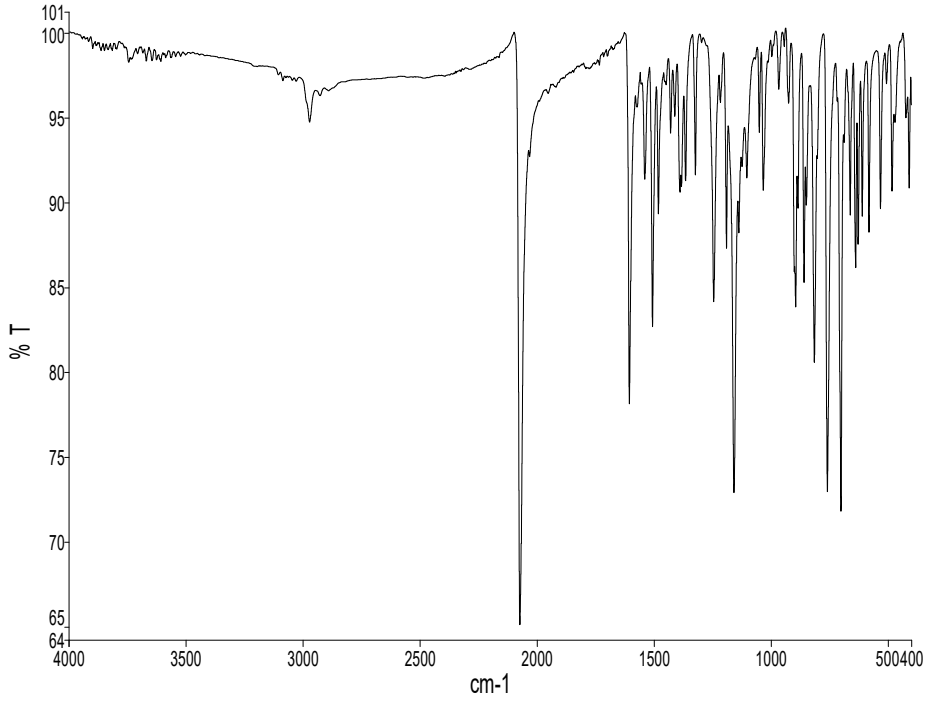

Figure. S26. The solid-state FT-IR spectrum of [{Co(**4**)$_2$(NCS)$_2$}·CHCl$_3$]$_n$.

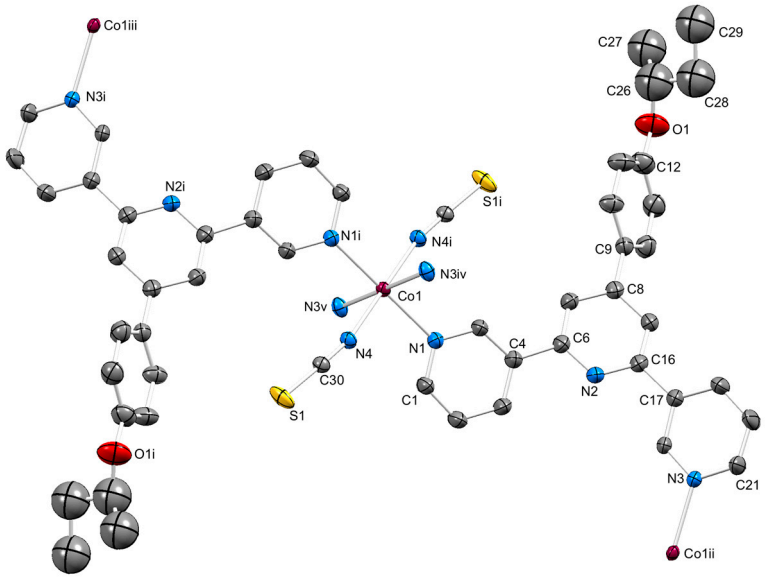

Figure. S27. ORTEP representation of the coordination sphere of atom Co1 (with symmetry generated Co centers) in [{Co(*rac*-**2**)$_2$(NCS)$_2$}·CHCl$_3$]$_n$ (symmetry codes: i = 1–*x*, 1–*y*, 1–*z*; ii = $^1/_2$–*x*, –$^1/_2$+*y*, $^1/_2$–*z*; iii = $^3/_2$–*x*, $^1/_2$+*y*, $^3/_2$–*z*; iv = $^1/_2$+*x*, $^1/_2$–*y*, $^1/_2$+*z*; v = $^1/_2$–*x*, $^1/_2$+*y*, $^1/_2$–*z*).

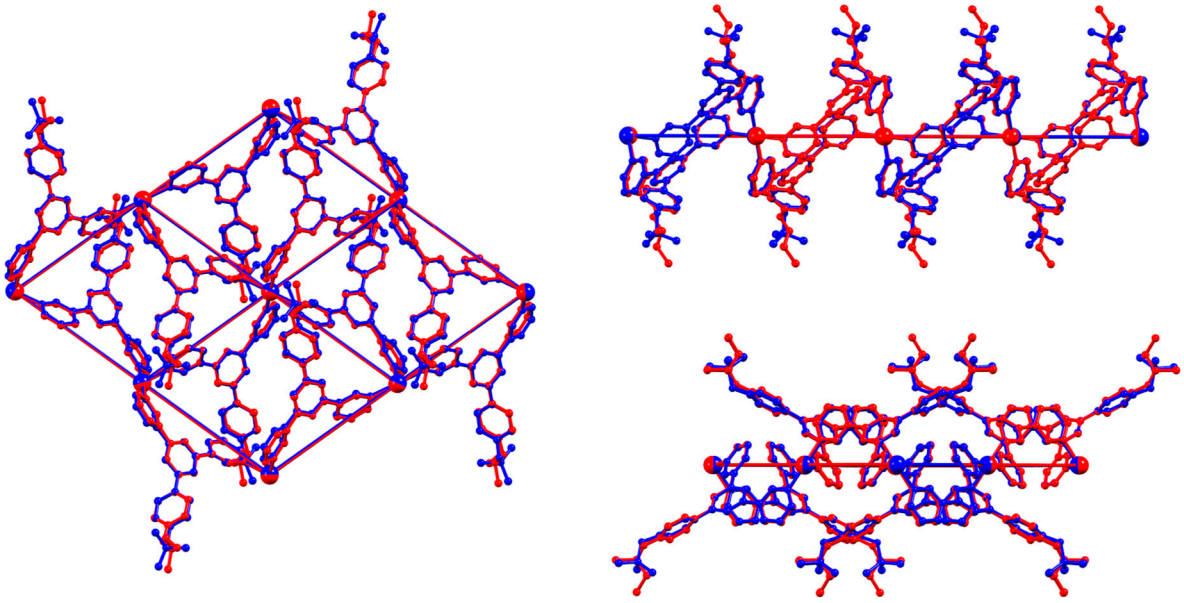

(a) (b)

Figure. S28. Overlays of parts of the (4,4) nets in $[\{Co(rac\text{-}\mathbf{2})_2(NCS)_2\}\cdot CHCl_3]_n$ (red) and $[\{Co(\mathbf{4})_2(NCS)_2\}\cdot CHCl_3]_n$ (blue).